BUCKLING ANALYSIS OF ANISOTROPIC THIN-WALLED CIRCULAR CYLINDRICAL SHELLS SUBJECT TO COMBINED LOADING

Esmaeal Ghavanloo [1] and S. Ahmad Fazelzadeh [2]

[1]School of Mechanical Engineering, Shiraz University, Shiraz 71963-16548, Iran
Email: ghavanloo@shirazu.ac.ir
[2]School of Mechanical Engineering, Shiraz University, Shiraz 71963-16548, Iran
Email: fazelzad@shirazu.ac.ir

Keywords: Circular cylindrical shell; Buckling; combined loading

Abstract
A continuum model is developed to study the buckling behavior of anisotropic thin-walled circular cylindrical shells under combined torsional load, axial compressive force and external radial pressure. In this paper, the governing equations are derived and analytical solution is presented for predicting the buckling behavior of the anisotropic thin-walled cylindrical shells subjected to combined loads by using the Flügge shell theory and complex method. To validate the accuracy of the results of this analysis, the results are compared with solutions found in the literature. It shows that the present model is accurate and appropriate for the prediction of buckling behavior of thin-walled cylindrical shells. Based on the present model, relationships between the critical pressure, axial and torsion loads are established, which can be used for determining the stress limits when designing practical systems in which combined loads may be applied.

1. Introduction

Thin-walled circular cylindrical shells are highly efficient structures and they have wide practical applications in the aerospace, petrochemical and construction industries [1]. When shells are subjected to the radial pressure, axial and torsional loads, their strengths are limited by structural buckling. Thus, the buckling of the shells under various types of combined loads has been subject of many investigations [2-5]. However, very little information has been published on triple-load interactions [6-9].
Motivated by the above ideas, we develop a continuum model to study the buckling behavior of anisotropic thin-walled cylindrical shells under combined torsional load, axial compressive force and external radial pressure. In this paper, the governing equations are derived and analytical solution is presented for predicting the buckling behavior of the anisotropic thin-walled cylindrical shells subjected to combined loads by using the Flügge shell theory and complex method. The Flügge theory is known as a highly reliable theory that can be used for most shapes regardless of the size of their cross-sectional radius. To validate the accuracy of the results of this analysis, the results are compared with solutions found in the literature. It shows that the present model is accurate and appropriate for the prediction of buckling behavior of thin-walled cylindrical shells. Based on the present model, relationships between the critical pressure, axial and torsion loads are established, which can be used for determining the stress limits when designing practical systems in which combined loads may be applied.

Excerpt from ISBN 978-3-00-053387-7

2. Mathematical Formulation of the Problem

The geometry of the shell and coordinate system are shown in Fig. 1. The cylindrical shell is assumed to have length *L*, and thickness *h*, and both ends of the shell are considered simply supported. In the case of circular cylindrical shell, we use *x* and θ as axial and circumferential angular coordinates, respectively, and *z* is the coordinate along thickness (outward) of the shell. The displacements in the axial, circumferential, and radial directions are denoted by *u*, *v*, and *w*, respectively. The governing equations for the thin-walled cylindrical shell with uniform external loads are [10, 11]

$$\frac{\partial N_{xx}}{\partial x}+\frac{1}{R}\frac{\partial \bar{N}_{x\theta}}{\partial \theta}-\frac{1}{2R^2}\frac{\partial \bar{M}_{x\theta}}{\partial \theta}-N\frac{\partial^2 u}{\partial x^2}-\frac{2T}{R}\frac{\partial^2 u}{\partial x\partial \theta}-pR\left(\frac{1}{R^2}\frac{\partial^2 u}{\partial \theta^2}-\frac{1}{R}\frac{\partial w}{\partial x}\right)=0 \tag{1}$$

$$\frac{1}{R}\frac{\partial N_{\theta\theta}}{\partial \theta}+\frac{\partial \bar{N}_{x\theta}}{\partial x}+\frac{3}{2R}\frac{\partial \bar{M}_{x\theta}}{\partial x}+\frac{1}{R^2}\frac{\partial M_{\theta\theta}}{\partial \theta}-N\frac{\partial^2 v}{\partial x^2}-\frac{2T}{R}\left(\frac{\partial^2 v}{\partial x\partial \theta}+\frac{\partial w}{\partial x}\right)-pR\left(\frac{1}{R^2}\frac{\partial^2 v}{\partial \theta^2}+\frac{1}{R^2}\frac{\partial w}{\partial \theta}\right)=0 \tag{2}$$

$$\frac{\partial^2 M_{xx}}{\partial x^2}+\frac{2}{R}\frac{\partial^2 \bar{M}_{x\theta}}{\partial x\partial \theta}+\frac{1}{R^2}\frac{\partial^2 M_{\theta\theta}}{\partial \theta^2}-\frac{N_{\theta\theta}}{R}-N\frac{\partial^2 w}{\partial x^2}-\frac{2T}{R}\left(-\frac{\partial^2 w}{\partial x\partial \theta}+\frac{\partial v}{\partial x}\right)-pR\left(\frac{1}{R^2}\frac{\partial^2 w}{\partial \theta^2}+\frac{1}{R}\frac{\partial u}{\partial x}-\frac{1}{R^2}\frac{\partial v}{\partial \theta}\right)=0 \tag{3}$$

where *N*, *T* and *p* are externally applied mid-face axial compressive force, torsional load and uniform external pressure, respectively. N_{xx}, $N_{\theta\theta}$, $\bar{N}_{x\theta}$ are force resultants and M_{xx}, $M_{\theta\theta}$, $\bar{M}_{x\theta}$ are moment resultants defined as

$$\{N_{xx}, N_{\theta\theta}, \bar{N}_{x\theta}\} = \int_{-\frac{h}{2}}^{\frac{h}{2}} \{\sigma_{xx}\left(1+\frac{z}{R}\right), \sigma_{\theta\theta}, \tau_{x\theta}\left(1+\frac{z}{R}\right)\} dz \tag{4}$$

$$\{M_{xx}, M_{\theta\theta}, \bar{M}_{x\theta}\} = \int_{-\frac{h}{2}}^{\frac{h}{2}} \{\sigma_{xx}\left(1+\frac{z}{R}\right)z, \sigma_{\theta\theta} z, \tau_{x\theta}\left(1+\frac{z}{R}\right)z\} dz \tag{5}$$

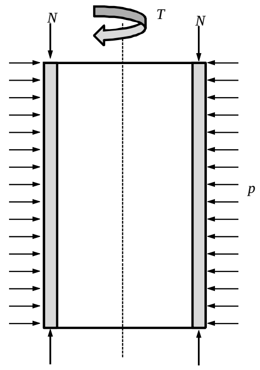

Figure 1. Geometry of thin-walled cylindrical shell under combined loads.

The strain components e_{xx}, $e_{\theta\theta}$ and $e_{x\theta}$ at an arbitrary point of the shell are related to the middle surface strains e_1, e_2 and e_3 and to the changes in the curvature of the middle surface k_1, k_2 and k_3 by the following relationships:

$$\{e_{xx}, e_{\theta\theta}, e_{x\theta}\} = \{e_1, e_2, e_3\} + z\{k_1, k_2, k_3\} \tag{6}$$

According to Flügge linear shell theory [12], the middle surface strain-displacement relationships and changes in the curvature for the circular cylindrical shell are

Excerpt from ISBN 978-3-00-053387-7

$$\{e_1,e_2,e_3\}=\{\frac{\partial u}{\partial x},\frac{1}{R}\frac{\partial v}{\partial \theta}+\frac{w}{R},\frac{\partial v}{\partial x}+\frac{1}{R}\frac{\partial u}{\partial \theta}\} \tag{7}$$

$$\{k_1,k_2,k_3\}=\{-\frac{\partial^2 w}{\partial x^2},-\frac{1}{R^2}\frac{\partial^2 w}{\partial \theta^2}-\frac{w}{R^2},-\frac{2}{R}\frac{\partial^2 w}{\partial x\partial \theta}-\frac{1}{R^2}\frac{\partial u}{\partial \theta}+\frac{1}{R}\frac{\partial v}{\partial x}\} \tag{8}$$

After the substitution of equations (4)-(8) into equations (1)-(3), the governing equations for the anisotropic thin-walled cylindrical shell in terms of axial, circumferential and radial displacements of the mean surface, (u, v, w), are obtained as:

$$\begin{aligned}
&[\frac{\partial^2}{\partial X^2}+\frac{c_{13}}{r}(2-\frac{3}{2}\frac{H^2}{12r^2})\frac{\partial^2}{\partial X\partial\theta}+\frac{c_{33}}{r^2}(1-\frac{H^2}{12r^2})\frac{\partial^2}{\partial\theta^2}]\,u^*+[c_{13}(1+\frac{H^2}{12r^2})\frac{\partial^2}{\partial X^2}+(\frac{c_{12}+c_{33}}{r})\frac{\partial^2}{\partial X\partial\theta}\\
&+\frac{c_{23}}{r^2}(1-\frac{H^2}{12r^2})\frac{\partial^2}{\partial\theta^2}]\,v^*+[\frac{c_{12}}{r}(1-\frac{H^2}{12r^2})\frac{\partial}{\partial X}+\frac{c_{23}}{r^2}(1-\frac{H^2}{12r^2})\frac{\partial}{\partial\theta}\\
&-\frac{H^2}{12r}\frac{\partial^3}{\partial X^3}-(\frac{c_{12}H^2+c_{33}H^2}{12r^3})\frac{\partial^3}{\partial X\partial\theta^2}-\frac{5}{2}\frac{c_{13}H^2}{12r^2}\frac{\partial^3}{\partial X^2\partial\theta}\\
&-\frac{c_{23}H^2}{24r^4}\frac{\partial^3}{\partial\theta^3}]\,w^*=N^*\left(\frac{\partial^2u^*}{\partial X^2}\right)+\frac{2T^*}{r}\left(\frac{\partial^2u^*}{\partial X\partial\theta}\right)+\frac{p^*r}{H}\left(\frac{1}{r^2}\frac{\partial^2u^*}{\partial\theta^2}-\frac{1}{r}\frac{\partial w^*}{\partial X}\right)
\end{aligned} \tag{9}$$

$$\begin{aligned}
&[c_{13}(1+\frac{3}{2}\frac{H^2}{12r^2})\frac{\partial^2}{\partial X^2}+(\frac{c_{33}+c_{12}}{r}-\frac{c_{33}H^2}{12r^3})\frac{\partial^2}{\partial X\partial\theta}+\frac{c_{23}}{r^2}(1-\frac{H^2}{12r^2})\frac{\partial^2}{\partial\theta^2}]\,u^*+[c_{33}(1+4\frac{H^2}{12r^2})\frac{\partial^2}{\partial X^2}\\
&+\frac{c_{23}}{r}(2+\frac{5}{2}\frac{H^2}{12r^2})\frac{\partial^2}{\partial X\partial\theta}+\frac{c_{22}}{r^2}\frac{\partial^2}{\partial\theta^2}]\,v^*+[\frac{c_{23}}{r}(1-\frac{H^2}{12r^2})\frac{\partial}{\partial X}+\frac{c_{22}}{r^2}(1-\frac{H^2}{12r^2})\frac{\partial}{\partial\theta}-\frac{5}{2}\frac{c_{13}H^2}{12r}\frac{\partial^3}{\partial X^3}\\
&-\frac{9}{2}\frac{c_{23}H^2}{12r^3}\frac{\partial^3}{\partial X\partial\theta^2}-(\frac{5c_{33}H^2+c_{12}H^2}{12r^2})\frac{\partial^3}{\partial X^2\partial\theta}-\frac{c_{22}H^2}{12r^4}\frac{\partial^3}{\partial\theta^3}]\,w^*=N^*\left(\frac{\partial^2v^*}{\partial X^2}\right)+\frac{2T^*}{r}\left(\frac{\partial^2v^*}{\partial X\partial\theta}+\frac{\partial w^*}{\partial X}\right)+\frac{p^*r}{H}\left(\frac{1}{r^2}\frac{\partial^2v^*}{\partial\theta^2}+\frac{1}{r^2}\frac{\partial w^*}{\partial\theta}\right)
\end{aligned} \tag{10}$$

$$\begin{aligned}
&[-\frac{c_{12}}{r}\frac{\partial}{\partial X}-\frac{c_{23}}{r^2}\frac{\partial}{\partial\theta}+\frac{H^2}{12r}\frac{\partial^3}{\partial X^3}+\frac{2c_{13}H^2}{12r^2}\frac{\partial^3}{\partial X^2\partial\theta}-\frac{c_{23}H^2}{12r^4}\frac{\partial^3}{\partial\theta^3}]\,u^*+[-\frac{c_{23}}{r}\frac{\partial}{\partial X}-\frac{c_{22}}{r^2}\frac{\partial}{\partial\theta}+2\frac{c_{13}H^2}{12r}\frac{\partial^3}{\partial X^3}\\
&+(\frac{c_{12}H^2+4c_{33}H^2}{12r^2})\frac{\partial^3}{\partial X^2\partial\theta}+\frac{3c_{23}H^2}{12r^3}\frac{\partial^3}{\partial x\partial\theta^2}]\,v^*+[-\frac{c_{22}}{r^2}-\frac{c_{22}H^2}{12r^4}\frac{\partial^2}{\partial\theta^2}-\frac{c_{22}H^2}{12r^4}\frac{\partial^4}{\partial\theta^4}-\frac{H^2}{12}\frac{\partial^4}{\partial X^4}\\
&-(\frac{2c_{12}H^2+4c_{33}H^2}{12r^2})\frac{\partial^4}{\partial X^2\partial\theta^2}-\frac{4c_{13}H^2}{12r}\frac{\partial^4}{\partial X^3\partial\theta}-\frac{4c_{23}H^2}{12r^3}\frac{\partial^4}{\partial X\partial\theta^3}]\,w^*\\
&=N^*\left(\frac{\partial^2w^*}{\partial X^2}\right)+\frac{2T^*}{r}\left(-\frac{\partial^2w^*}{\partial X\partial\theta}+\frac{\partial v^*}{\partial X}\right)+\frac{p^*r}{H}\left(\frac{1}{r^2}\frac{\partial^2w^*}{\partial\theta^2}+\frac{1}{r}\frac{\partial u^*}{\partial X}-\frac{1}{r^2}\frac{\partial v^*}{\partial\theta}\right).
\end{aligned} \tag{11}$$

where

$$\begin{aligned}
&X=\frac{x}{L} \qquad u^*=\frac{u}{L} \qquad v^*=\frac{v}{L} \qquad w^*=\frac{w}{L} \qquad r=\frac{R}{L} \qquad H=\frac{h}{L}\\
&c_{ij}=\frac{C_{ij}}{C_{11}}=\frac{12D_{ij}}{H^3L^2} \qquad N^*=\frac{N}{C_{11}HL} \qquad T^*=\frac{T}{C_{11}HL} \qquad D_{ij}=\frac{C_{ij}h^3}{12} \qquad p^*=\frac{p}{C_{11}}
\end{aligned} \tag{12}$$

in which C_{ij} are the components of elastic constants. Up to now, the analysis has been general without reference to the boundary conditions. An analytical solution based on complex method is presented for analyzing the buckling behavior of the anisotropic thin-walled cylindrical shells with a special boundary condition. Complex variable is used to solve the governing equations (9)-(12) by setting the real and imaginary zero. This is commonly used as solution technique to solve differential equations of coupling problems in mathematics [13]. For simply supported boundary condition, we have Re (w^*) = Re (v^*) = 0 at both ends of shells. The displacement fields that satisfy these essential boundary conditions at x = 0, L can be written as:

$$u^*=\overline{U}\exp(i\lambda_q X)\cos(n\theta) \tag{13}$$

$$v^*=-i\overline{V}\exp(i\lambda_q X)\sin(n\theta) \tag{14}$$

$$w^*=-i\overline{W}\exp(i\lambda_q X)\cos(n\theta) \tag{15}$$

where $\bar{U}$, $\bar{V}$ and $\bar{W}$ are the non-dimensional displacement amplitudes in the x, θ, z directions, respectively, λ_q ($\lambda_q = m\pi$, m is the half-axial wave-number) is the wave-number along the axial direction, n is the wave-number in the circumferential direction. This displacement field provides us a good way to solve the couple problems. It has at least three features: it satisfies the partial differential equations; it easily satisfies the boundary conditions because it is in form of sine and cosine functions; it takes account into the interactive effect of coordinates of x and θ when substituting the governing equations and setting the real and imaginary zero. Substituting equations (13)-(15) into equations (9)-(11), yields a set of algebraic equations for $\bar{U}$, $\bar{V}$ and $\bar{W}$ as

$$\mathbf{E}(m,n,N^*,T^*,p^*)_{3\times 3}\begin{bmatrix}\bar{U}\\ \bar{V}\\ \bar{W}\end{bmatrix}=\begin{bmatrix}0\\0\\0\end{bmatrix} \quad (16)$$

Here [**E**] is a nonsymmetric matrix. For the non-trivial solution, the determinant of this set of equations must be zero, i.e.

$$\det \mathbf{E}(m,n,N^*,T^*,p^*)_{3\times 3}=0 \quad (16)$$

By solving the resulting eigenvalue problem, the critical buckling loads of the cylindrical shells can be obtained and the associated eigenvectors yields the corresponding mode shapes. For elastic buckling analysis, we search for the minimum load.

3. Numerical Results and Discussion

To check the validity, efficiency, and accuracy of the present method, some comparisons of the results are made for various loading conditions. In Table 1, the non-dimensional critical axial compressive forces are given for an isotropic thin cylindrical shell and compared with the values determined based on the formulation given by Yoo and Lee [14]. The results in Table 1 indicate that the present results are consistent with those available in the literature. Table 2 compares the results for non-dimensional critical pressure of thin cylindrical shell with simply supported boundary conditions with the results of Yoo and Lee [14]. It may be noted here that the solutions obtained for this case using the present model agree well with those of analytical approach [14].

The effect of the external pressure on the axial stability of the thin-walled cylindrical shells is investigated. Fig. 2 presents the effect of the external pressure on the critical axial compressive load of the isotropic cylindrical shell with different values of the aspect ratio. For numerical simulation purpose, the following parameters are used: r/H = 20, ν = 0.3 and T^* = 0. As it is observed, the aspect ratio plays an important role in indicating how the external pressure affects the mechanism of the buckling. It can also be seen that with increasing the aspect ratio, (decreasing of r), the stable region (under the critical curve) is reduced. In addition, any increase in the external pressure decreases the critical axial compressive load of the cylindrical shells. In fact, in this case, the external pressure pushes the wall of cylinder inward, resulting in a stronger tendency of the cylinder to collapse under axial compressive load.

As the second case, the effect of the anisotropic properties of the shell on its buckling behavior is shown in Fig. 3. The anisotropic properties of four materials, which are used in this work, are given in Table 3. In this case, we take H = 0.025, r = 0.5 and T^* = 0.

Finally, we consider the buckling of cylindrical shells subjected to combinations of three loadings: axial compression force, torsion load and external internal pressure. Fig. 5 shows the effect of the external pressure and the applied torque on the critical axial compressive loads of the cylindrical shell made of material 3. For numerical simulation purpose, the following parameters are used: r/H = 20 and r = 0.1. Similar to the effect of the external pressure and the torque on the critical axial compressive force, the existence of the external pressure and the torque result in a lower critical buckling axial compressive force than the corresponding one under pure axial buckling. This figure can be used for determining the load limits when designing thin-walled cylindrical shell in which combined loads may be applied.

Table 1. Comparison between non-dimensional critical axial compressive force, N^*, of cylindrical shell obtained from present simulations and Yoo and Lee [14] for v=0.3.

		r = 2	H = 0.01	r = 2	H = 0.05
m	n	Yoo and Lee [14]	Present	Yoo and Lee [14]	Present
1	1	0.0220	0.0219	0.0239	0.0239
1	2	0.0191	0.0189	0.0213	0.0212
1	3	0.0154	0.0152	0.0181	0.0180
1	4	0.0118	0.0116	0.0154	0.0153
1	5	0.0088	0.0087	0.0136	0.0137
2	1	0.0060	0.0060	0.0133	0.0140
2	2	0.0058	0.0058	0.0133	0.0141
2	3	0.0055	0.0055	0.0135	0.0143
2	4	0.0051	0.0051	0.0138	0.0146
2	5	0.0047	0.0047	0.0143	0.0152
3	1	0.0032	0.0033	0.0195	0.0211
3	2	0.0032	0.0033	0.0197	0.0214
3	3	0.0031	0.0032	0.0201	0.0218
3	4	0.0031	0.0031	0.0207	0.0225
3	5	0.0030	0.0031	0.0215	0.0234

Table 2. Comparison between non-dimensional critical pressure, p^*, of cylindrical shell obtained from present simulations and Yoo and Lee [14] for v=0.3.

H	R	Yoo and Lee [14]	Present	m	n
0.05	0.5	16.8572×10^{-4}	16.8955×10^{-4}	1	3
	1	6.5243×10^{-4}	6.532×10^{-4}	1	5
	2	2.6349×10^{-4}	2.6329×10^{-4}	1	9
0.01	0.5	0.2599×10^{-4}	0.2559×10^{-4}	1	5
	1	0.0964×10^{-4}	0.0961×10^{-4}	1	8
	2	0.0567×10^{-4}	0.0571×10^{-4}	1	10

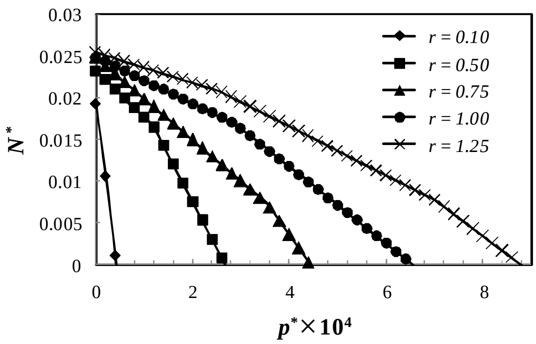

Figure 2. Critical axial compressive loads of isotropic cylindrical shell versus the external pressure for different values of r.

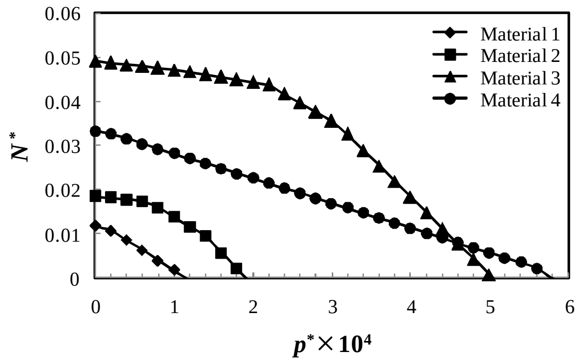

Figure 3. Critical axial compressive loads of four anisotropic cylindrical shells versus the external.

Table 3. Material properties of four anisotropic materials.

	Elastic constants				
	c_{22}	c_{12}	c_{13}	c_{23}	c_{33}
Material 1	0.34	0.10	0.00	0.00	0.14
Material 2	0.54	0.29	0.29	0.10	0.35
Material 3	1.85	0.52	0.20	0.54	0.64
Material 4	2.95	0.27	0.00	0.00	0.40

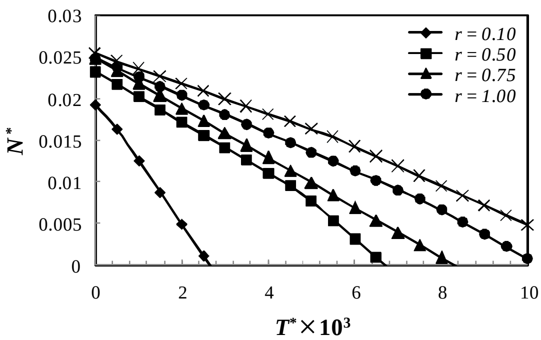

Figure 4. Critical axial compressive loads of isotropic cylindrical shell versus the torque for different values of *r*.

3. Conclusions

In this work, the combined effects of external loads on the buckling properties of the anisotropic cylindrical shell under combined loads was studied. In spite of some achievement in the buckling analysis of the cylindrical shells, to the authors' knowledge, there has been no attempt to tackle the problem described in the present investigation. The validity of the results was successfully verified through comparison with data available in the literature. The main results of the present work are summarized as follows.

1) Under combined loads, the stable region is reduced when the aspect ratio of the shell is increased.
2) Application of the external pressure and applied torque result in a lower critical axial buckling than the corresponding one under pure axial buckling.

Excerpt from ISBN 978-3-00-053387-7

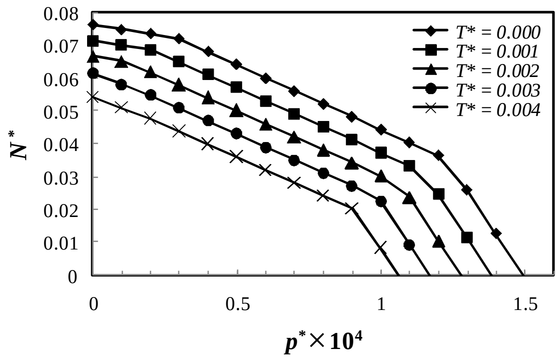

Figure 5. Buckling of anisotropic cylindrical shells under combined loads.

References

[1] F. Alijani and M. Amabili. Non-linear vibrations of shells: A literature review from 2003 to 2013. Int. J. Non-Lin. Mech., 58: 233-257, 2014.

[2] G. Kirshnamoorthy. Buckling of thin cylinders under combined external pressure and axial compression. *J. Aircraft*, 11: 65-68, 1974.

[3] C.G. Foster. Interaction of buckling modes in thin-walled cylinders. *Exp. Mech.*, 21: 124-129, 1981.

[4] X. Wang, G.X. Lu and Y.J. Lu. Buckling of embedded multi-walled carbon nanotubes under combined torsion and axial loading. *Int. J. Solids Struct.*, 44: 336-351, 2007.

[5] C. Sun and K. Liu Combined torsional buckling of multi-walled carbon nanotubes coupling with axial loading and radial pressures. *Int. J. Solids Struct.*, 45: 2128-2139, 2008.

[6] H. Allahbakhsh and M. Shariati. Instability of cracked CFRP composite cylindrical shells under combined loading. *Thin-Wall. Struct.*, 74: 28-35, 2014.

[7] J. Arbocz. The effect of imperfect boundary conditions on the collapse behavior of anisotropic shells. *Int. J. Solids Struct.*, 37: 6891-6915, 2000.

[8] J. Sun, X.S. Xu and C.W. Lim. Symplectic method for dynamic buckling of cylindrical shells under combined loading. *Int. J. Appl. Mech.*, 5: 1350042, 2013.

[9] T.A. Winterstetter and H. Schmidt. Stability of circular cylindrical steel shells under combined loading. *Thin-Wall. Struct.*, 40:893-910, 2002.

[10] W. Flügge. *Stresses in Shells*. Springer, 1960.

[11] B. Gu, Y.W. Mai and C.Q. Ru. Mechanics of microtubules modeled as orthotropic elastic shells with transverse shearing. *Acta Mech.*, 207: 195-209, 2009.

[12] M. Amabili. *Nonlinear Vibrations and Stability of Shells and Plates*. Cambridge University Press, 2008.

[9] K.Y. Lam and W. Qian. Free vibration of symmetric angle-ply thick laminated composite cylindrical shells. *Compos. Part B*, 31: 345-354, 2000.

[10] C.H. Yoo and S.C. Lee. *Stability of Structures*. Elsevier, 2011.

Excerpt from ISBN 978-3-00-053387-7